An Electric Bottle for Colloids

M. T. Sullivan,[1] K. Zhao,[1] A. D. Hollingsworth,[2] R. H. Austin,[1] W. B. Russel,[2] and P. M. Chaikin[1]
[1]*Department of Physics, Princeton University, Princeton, New Jersey 08544, USA*
[2]*Department of Chemical Engineering, Princeton University, Princeton, New Jersey 08544, USA*

(Received 11 December 2004; published 9 January 2006)

Particle concentration is a dominant control parameter for colloids and other soft matter systems. We demonstrate a simple technique, "dielectrophoretic equilibrium," implemented as an "electric bottle," a planar capacitor in a larger volume. The uniform E field in the capacitor traps particles in this force-free region at a higher density than in the zero field regions outside. We show how the technique measures the equation of state and we initiate and grow colloidal crystals. "Dielectrophoretic equilibria" enable the study of a complete concentration-dependent phase diagram from a single microscopic sample, obviating the previous need for preparing a large number of samples.

DOI: 10.1103/PhysRevLett.96.015703 PACS numbers: 82.70.Dd

In a uniform electric field E neutral particles of volume v_p lower their energy by $-(\varepsilon_{\text{eff}}E^2/2)v_p$, but feel no net force. The effective dielectric constant ε_{eff} is an interesting function of the complex frequency-dependent conductivity or dielectric constant of the particle and solvent. If ε_{eff} is positive then from statistical mechanics the particle density will be higher in a region of higher field. That is the simple principle we exploit. In a field gradient, the particles experience a force $\nabla(-\varepsilon_{\text{eff}}E^2/2)v_p$ and undergo motion, called dielectrophoresis. Dielectrophoresis has been used in many ways to control the behavior of colloidal particles, for particle separation, characterization, and transport [1,2]. Typically, such work has been used in dilute suspensions to move and sort individual colloidal particles or small groups of such particles. The difference between conventional dielectrophoresis and the present technique is that we use a finite system and let it come to equilibrium with the osmotic pressure balancing the electrostatic driving force. Equivalently we may view the energy $-\varepsilon_{\text{eff}}E^2/2$ as an additional term in the particle chemical potential, μ. The requirement of constant μ in a system with open particle exchange then lowers the concentration in the low field region relative to the high field region.

To test and quantify these ideas we have performed experiments with a suspension of poly(methylmethacrylate) colloids. The particles are sterically stabilized with PHSA (polyhydoxystearic acid) and suspended in near index matching solvents. Such systems behave as hard spheres [3–5]. To prevent sedimentation, which would also induce density gradients, the suspensions have been formulated in a density matching mixture of decahydronaphthalene and tetrachloroethylene. The particles have been dyed with Rhodamine 6G for fluorescence confocal microscopy. Hard spheres are particularly appropriate for this study as well as interesting in their own right. With only an excluded volume repulsive interaction and no attractive interaction, their phase behavior is entirely controlled by the volume fraction, ϕ. Below $\phi = 0.494$, the dispersion assumes an isotropic fluid phase, above $\phi = 0.545$ the system is crystalline, and for $0.494 < \phi < 0.545$ the two phases coexist. For slightly polydisperse samples in normal gravity a glass phase exists above $\phi \sim 0.58$ [5,6]. Gravity and temperature gradients have previously been used to measure interactions and control density. A comparison with preliminary dielectrophoretic studies is found in Ref. [7].

Experiments in a confocal microscope require only microscopic sample quantities. Furthermore, equilibration times are relatively short, high fields are available at low voltages, and there is an extensive literature for determining structure and particle density [7]. Our cell configuration is shown schematically in Fig. 1. A capacitor is formed by evaporating thin transparent electrodes (200 Å Au/20 Å Cr for data shown below) spanning $\sim 1/3$ of the cell area. For insulating samples the electrodes can be either in contact with the suspension or outside the cover slip (shown). The cell is filled with a suspension having an initial average volume fraction appropriate for the region of the phase diagram of interest (e.g., liquid, crystal-liquid, glass-crystal).

Figure 2 shows the results for a sample at an initially low fraction ($\phi \sim 0.12$). As expected, the particles have become dense in the central region, are sparse outside the capacitor plates, and show a sharp density gradient near the edge of the capacitor. The particle number is measured using confocal microscopy and particle tracking algorithms and converted to a volume fraction by comparing with a sample of known volume fraction. Scanning across the entire length of the cell yields a volume fraction profile. The observed density profile and that predicted from statistical mechanics with measured properties of the particles and solvent (no adjustable parameters) are shown in the lower left for two different fields. Calculated and measured profiles agree remarkably well. Of particular interest here is that the agreement is equally good over a factor of 2 change in applied field. As discussed later, this implies that the equation of state and the interparticle correlation func-

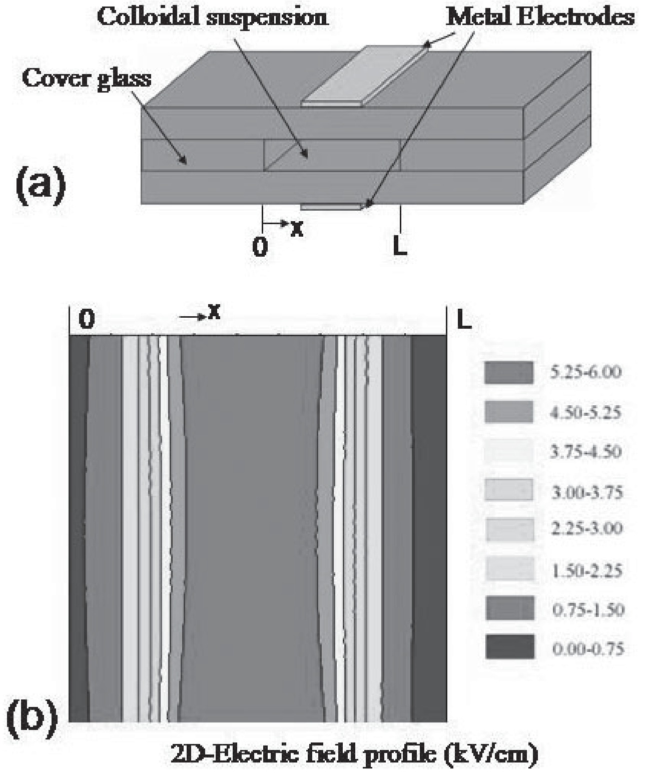

FIG. 1. (a) Schematic of an "electric bottle," constructed with microscope slides and cover slips. (b) Midplane field profile calculated for a typical experimental cell as shown in (a).

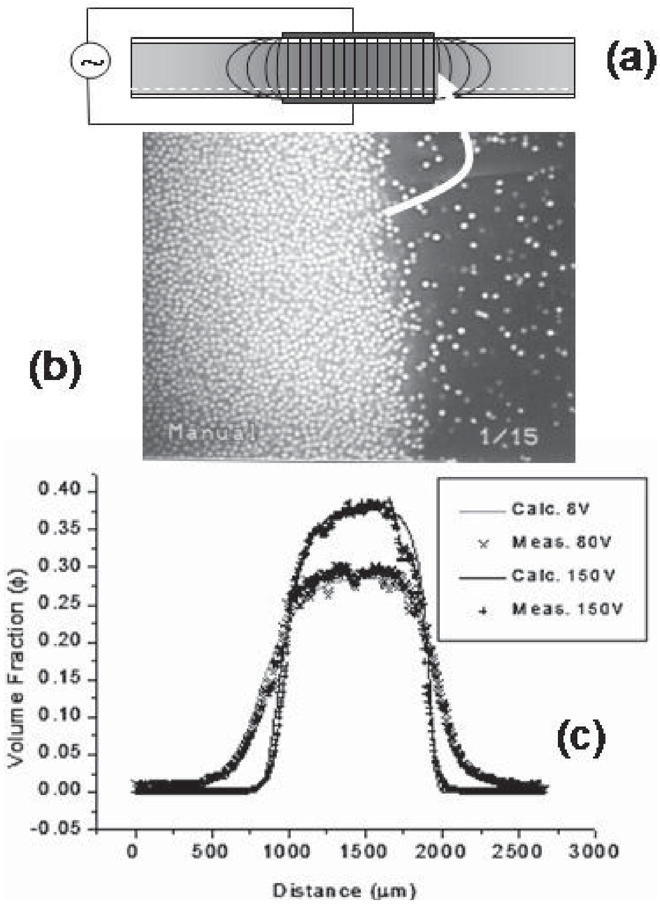

FIG. 2. Equilibrium properties of a cell filled initially with a volume fraction $\phi \sim 0.12$. (a) Cell schematic. (b) Confocal micrograph of the region near the strong field gradient after 24 h, with the maximum field at 6 kV/cm. There is a steplike change between the constant high and low density regions. In both regions the particles undergo Brownian motion and there is no net particle flow. (c) The plots (displaced for clarity) show the measured (points) and calculated (lines) particle volume fraction profiles. Sharper data are for 150 volts applied across the 0.480 mm cell, broader data for 80 V. The calculated lines have no free parameters. The asymmetry is due to the measured misalignment of upper and lower electrodes.

tion are not significantly changed from their zero field values.

In denser samples ($\phi \sim 0.50$), we can control crystal formation, Fig. 3. Just as before, the density increases in the central region, but now the densification pushes the volume fraction above the freezing point and crystals form. There is a sharp interface between the liquid and crystalline regions evident in both the confocal microscope image, which shows particles with crystalline order adjacent to the disordered liquid, and in the macroscopic image, which shows the Bragg scattering from the well-defined crystallites adjacent to the diffusely scattering liquid. Measurements of the concentration profile agree with predictions in this concentration region as well. The observed crystal structure is random hexagonally close packed, as is seen in other hard sphere experiments. When the electric field is turned off, the sample relaxes to coexistence between the central crystal region with volume fraction $\phi = 0.545$ and a surrounding fluid phase with $\phi = 0.494$. This separation is thermodynamically stable, so the system is observed to remain separated for at least a month after the removal of the electric field. Typically in a coexistence sample, small crystallites nucleate and grow. Here, we have been able to control the stable crystal-liquid interface.

The calculation of the particle density profile requires knowledge of the dielectric constant of the particles, ε_p, and solvent, ε_m (at the applied frequency), and the equation of state. At very low particle density and field $\varepsilon_{\mathrm{eff}}$ is given by the Clausius-Mossetti equation [$\varepsilon_{\mathrm{eff}} = 3\beta\varepsilon_m$, $\beta = (\varepsilon_p - \varepsilon_m)/(\varepsilon_p + 2\varepsilon_m)$], the electric field is that from a capacitor with spatially uniform dielectrics, and the interparticle interactions from the induced dipoles are negligible. In this case the ratio of in/out particle density is just given by $\mu = \mathrm{const} = kT\ln(n_{\mathrm{out}}) = kT\ln(n_{\mathrm{in}}) - \varepsilon_{\mathrm{eff}}E^2 v_p/2$ which produces the simple Boltzmann result $(n_{\mathrm{in}}/n_{\mathrm{out}}) = \exp(-\varepsilon_{\mathrm{eff}}E^2 v_p/2kT)$. Thus, the density profile depends exponentially on the field profile. For a more concentrated suspension and/or higher fields, interparticle interactions become important, and the electric field must be calculated self-consistently in terms of the spatially varying suspension dielectric constant [8] which in turn depends on the local field and the induced interparticle interactions.

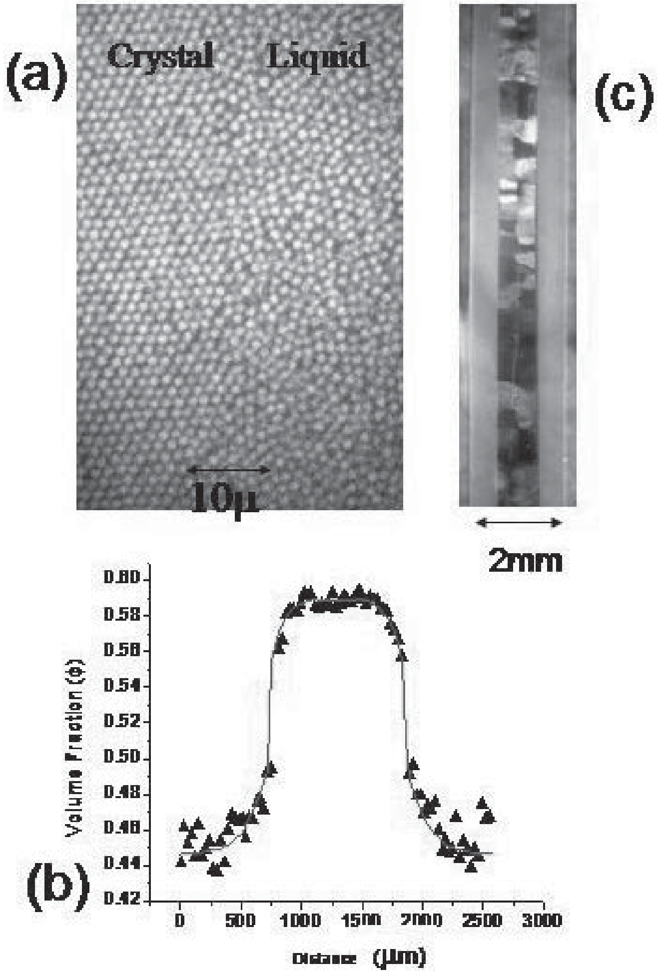

FIG. 3. Equilibrium properties of a cell filled initially to $\phi \sim 0.50$. (a) Confocal micrographs of the interface between crystal and liquid phases. (b) Measured and calculated volume fraction profile. (c) Low magnification optical image shows Bragg scattering from crystallites under electrodes and diffuse scattering from liquid in lower density region outside the electric "bottle."

Fortunately, for aligned dipoles in spherical, cubic, and hexagonal symmetry the dipole-dipole interaction averages to zero. If the electric field is small enough to leave the symmetry unchanged, the only energy that needs to be taken into account is the macroscopic electrostatic energy difference, $\varepsilon_{\mathrm{eff}}(\phi)E^2/2$. The effective dielectric constant depends on the underlying particle structure, but rigorous bounds on its possible value [9] exist. For systems with small dielectric mismatch we can approximate the effective particle dielectric constant as $\varepsilon_{\mathrm{eff}}(\phi) = 3[\beta\varepsilon_m/(1-\beta\phi)^2]$ [11]. Given the voltage on the capacitor and the spatial distribution of particles, we can calculate numerically the electric field in the cell. The requirement of constant chemical potential and the hard sphere chemical potential calculated from the liquid and crystalline equation of state [12,13] allow us to calculate the induced density profile given the electric field. We can then iteratively calculate the electric field and concentration profiles until all are stationary. The calculated curves in Fig. 2 were obtained by this iteration with no adjustable parameters.

The above procedure uses information on the equation of state to obtain the density profile. The inverse problem is much more straightforward. If we measure the density profile $\phi(x)$, we know the local value of the suspension dielectric constant $\varepsilon_s[\phi(x)] \sim \varepsilon_m(1-\phi) + \varepsilon_p\phi$ without iteration [9]. Chemical potential equilibrium then directly yields the equation of state. Unfortunately the sharp field gradient at the edge of the capacitor makes evaluation difficult in this geometry. A wedge geometry of plates would be more appropriate. For the simple capacitor arrangement in the present experiment the equation of state can be obtained by changing the voltage on the plates.

We have neglected the possibility that field induced forces will change the symmetry from spherical or cubic. The amplitude of such a distortion would be proportional to the dipole-induced stress over an elastic constant G, $\varepsilon_{\mathrm{eff}}E^2/G$. This would unbalance the cancellation of induced dipolar forces and lead to an energy decrease [14] of order $\varepsilon_{\mathrm{eff}}{}^2E^4/G$. Experimentally we can easily tell whether this term is significant by looking for nonlinearities in E^2 by changing the applied voltage. As we have seen in Fig. 2 the fit to a simple hard sphere equation of state does not change with E over the field range studied. For much higher fields the structure will indeed change and eventually give rise to chains of dipoles characteristic of electrorheological fluids [15].

Gravity [16,17] and temperature gradients [18] have previously been used to produce density profiles in colloidal systems, but neither allows the precise control available with electric fields. Dielectrophoretic equilibrium is applicable to many soft condensed matter systems. For $E = 1000$ V/cm, the energy density $\varepsilon_0E^2/2 \sim 0.44$ dynes/cm^2 is comparable to elastic constants and pressures in systems with characteristic interparticle spacing or unit cell dimensions of $L \sim 1$ micron (i.e., $k_BT/L^3 \sim \varepsilon_0E^2/2$). Such easily attainable fields should be useful in controlling not only density but composition (of particle mixtures) and orientation (of anisotropic particle and crystals) and in directing self-assembly processes (e.g., nucleation and growth). Combined with flow fields in microfluidic devices the dielectrophoretic steady state can be used for separations. The fact that $\varepsilon_{\mathrm{eff}}$ is also controllable with frequency in aqueous and electrolyte suspensions (to the extent that the sign is even reversible), and that the field can be varied with time, creates the potential for controlling and measuring submicron scale architectures.

---

[1] H. A. Pohl, *Dielectrophoresis: The Behavior of Neutral Matter in Non-Uniform Electric Fields* (Cambridge University Press, Cambridge, England, 1978).
[2] N. G. Green and H. J. Morgan, J. Phys. D **30**, L41 (1997).
[3] B. J. Adler and T. E. Wainwright, J. Chem. Phys. **27**, 1208 (1957).

[4] P. N. Pusey and W. van Megen, Nature (London) **320**, 340 (1986).

[5] P. N. Pusey, Course 10 in *Liquids, Freezing and the Glass Transition*, edited by J. P. Hansen, D. Leveesque, and J. Zinn-Justin (Elsevier, New York, 1991), p. 763.

[6] W. van Megen and S. M. Underwood, Phys. Rev. E **49**, 4206 (1994).

[7] Matt Sullivan, Kun Zhao, Christopher Harrison, Robert H. Austin, Mischa Megens, Andrew Hollingsworth, William B. Russel, Zhengdong Cheng, Thomas Mason, and P. M. Chaikin, J. Phys. Condens. Matter **15**, S11 (2003).

[8] The local coarse grained dielectric constant increases as the volume fraction of higher dielectric particles increases.

[9] For a two-component system with volume fraction ϕ of a dielectric material ε_p in a surrounding material ε_m, the suspension dielectric constant is bounded by

$$\left(\frac{1-\phi}{\varepsilon_m}+\frac{\phi}{\varepsilon_p}\right)^{-1} \le \varepsilon_s(\phi) \le \varepsilon_m(1-\phi)+\varepsilon_p\phi.$$

For an isotropic system or one with cubic point symmetry, tighter rigorous bounds exist on the macroscopic effective dielectric constant [10]:

$$\varepsilon_m + \frac{\phi}{(\varepsilon_p-\varepsilon_m)^{-1}+(1-\phi)/3\varepsilon_m} \le \varepsilon_s(\phi) \le \varepsilon_p + \frac{(1-\phi)}{(\varepsilon_m-\varepsilon_p)^{-1}+\phi/3\varepsilon_p}.$$

For small dielectric mismatches, this range is small. For our system, the maximum total range is less than 1.5% and less than 0.06% assuming isotropy. Thus, it is reasonable to approximate the dielectric constant at low fields, where the suspension should be isotropic, by the isotropic lower bound.

[10] Z. Hashin and J. Shtrikman, J. Appl. Phys. **33**, 3125 (1962).

[11] The expression in Ref. [9] is for the effective *suspension* dielectric constant—the overall dielectric constant of both the particles and suspension. The statistical condition for equilibrium is $\mu = \mu_0(\phi) - \nu_p \frac{\partial W}{\partial \phi} = \text{const}$, where $W = \frac{1}{2}[\varepsilon_s(\phi) - \varepsilon_m]|E|^2$ is the macroscopic electrostatic energy, in terms of the effective suspension dielectric constant $\varepsilon_s(\phi)$, and $\mu(\phi)$ is the internal chemical potential. The effective particle dielectric constant $\varepsilon_{\text{eff}}(\phi)$ is the coefficient that determines the electrostatic free energy for a single particle $\nu_p \frac{\partial W}{\partial \phi} = \nu_p \frac{3\beta\varepsilon_m}{(1-\beta\phi)^2}E^2/2 = \nu_p \varepsilon_{\text{eff}} E^2/2$. This effective particle dielectric constant accounts for particle-particle interactions and allows the single-particle force equation to be used in place of one that explicitly accounts for the surrounding medium.

[12] N. F. Carnahan and K. E. Starling, J. Chem. Phys. **51**, 635 (1969).

[13] K. R. Hall, J. Chem. Phys. **57**, 2252 (1972).

[14] The electrostatic energy for two interacting point dipoles is $u_{DD}(\vec{r}) = \frac{9\nu_p^2\varepsilon_m\beta^2E^2(1-3\cos^2\theta)}{4\pi r^3}$. The isotropy of the pair-distribution function assures the dipole-dipole interaction energy will integrate to zero for all terms of $O(E^2)$. The dipole-dipole interaction will cause an anisotropy, which, as long as it is small, can be approximated by perturbing the hard sphere pair-distribution function $g(\vec{r}) \approx g_{hs}(r) \times (1 - \frac{u_{DD}(\vec{r})}{k_BT})$. The resulting osmotic pressure is $\frac{\Pi}{k_BT} = \phi - \frac{\phi^2}{6k_BT}\int ru'(\vec{r})g(\vec{r})d\vec{r}$ which, when removing the hard sphere contribution, gives an osmotic pressure change from the isotropic case of $\frac{\Delta\Pi}{k_BT} \approx -\frac{27}{20}\phi^2(\frac{\nu_p\varepsilon_m\beta^2E^2}{k_BT})^2\int_1^\infty \frac{g_{hs}(s)ds}{s^4}$. Anisotropic contributions to the osmotic pressure will vary as E^4, just as in the crystalline case.

[15] P. M. Adriani and A. P. Gast, Phys. Fluids **31**, 2757 (1988).

[16] T. Biben, R. Ohnesorge, and H. Lowen, Europhys. Lett. **28**, 665 (1994).

[17] M. A. Rutgers, J. H. Dunsmuir, J.-Z. Xue, W. B. Russel, and P. M. Chaikin, Phys. Rev. B **53**, 5043 (1996); R. Piazza, T. Bellini, and V. Degiorgio, Phys. Rev. Lett. **71**, 4267 (1993).

[18] Z. Cheng, W. B. Russel, and P. M. Chaikin, Nature (London) **401**, 893 (1999).